Phase transformation properties of finite size ferroelectric thin film with structural transition zones

Jing Zhou,[1] Tianquan Lü,[1,a)] Lian Cui,[1] Hui Chen,[1] and Wenwu Cao[1,2]
[1]*Center of Condensed Matter Science and Technology, Harbin Institute of Technology, Harbin 150001, China*
[2]*Materials Research Institute, The Pennsylvania State University, University Park, Pennsylvania 16802, USA*

(Received 9 July 2008; accepted 3 November 2008; published online 17 December 2008)

By considering structural transition zones in the lateral and thickness directions of finite size ferroelectric thin film, phase transformation properties of the thin film are investigated based on a transverse Ising model. The influence of the lateral size of the thin film on the polarization and the Curie temperature has been quantified. Our results indicate that the lateral size of the film plays a crucial role in determining the phase transformation properties for a small size ferroelectric thin film. © *2008 American Institute of Physics*. [DOI: 10.1063/1.3043584]

I. INTRODUCTION

Ferroelectric thin films have triggered great interest due to recent progress in thin film based electronic devices, such as nonvolatile memories and field-effect transistors.[1] In view of the sustained trend toward further miniaturization of electronic devices, the investigation of surface and size effects in ferroelectric thin films is practically important. There have been a lot of experimental[2–10] and theoretical[11–26] efforts devoted to study these important effects.

Experimentally, an anomalous polarization pattern was reported by Stolichnov *et al.*[2] using scanning force microscopy across partially etched $Pb(Zr,Ti)O_3$ ferroelectric thin film having the size of 2×3 μm^2 with preferential orientation along (111). Interestingly, the thin film of the same texture with the size of 0.5×0.5 μm^2 and preferential orientation along (100) does not exhibit such an anomalous polarization distribution. Recently, Kim *et al.*[3] observed the retention characteristics of $(Bi,La)_4Ti_3O_{12}$ (BLT) film and their lateral (along the surface of film) size effect in a fully integrated device structure. Their experimental results showed that the retention characteristics of BLT capacitors have no degradation due to the size reduction down to 0.49×0.64 μm^2, which can be used for highly integrated ferroelectric random access memories of 32 Mbit density.

Theoretically, various approaches, including Ginzburg–Landau–Devonshire (GLD) theory,[11–15] first principles calculations[16,17] and transverse Ising model (TIM) (Refs. 18–26) have been adopted to study the surface and size effects in ferroelectrics. Using the GLD thermodynamic theory, the lateral size dependence of the Curie temperature and the polarization was obtained by Wang *et al.*[11] for a ferroelectric thin film with finite cells in three dimensions. It is demonstrated that the Curie temperature and the mean polarization of the film decrease with the reduction in the cell size. Based on *ab initio* calculations, Naumov *et al.*[16] investigated ferroelectric nanoscale disks and rods of $Pb(Zr,Ti)O_3$ solid solutions and reported the existence of unusual phase transitions in zero-dimensional ferroelectric nanoparticles. On the microscopic level, the pseudospin theory based on the traditional TIM is widely used. Despite its simplicity, the TIM is successful in studying ferroelectric properties of finite-size ferroelectrics. Wesselinowa and Trimper[18] applied the Green's function technique to a modified TIM to investigate the dielectric properties of the ferroelectric thin film. It is shown that the maximum of the dielectric constant decreases with the reduction in the film thickness. The phase transition temperature, at which the dielectric constant reaches a maximum, may decrease or increase depending on the strength of the surface transverse field and the exchange interaction. Xiong *et al.*[19] discussed the effects of exchange interaction and transverse field on the phase diagrams of the ferroelectric thin film with two surface layers. The results show that the phase transformation properties can be greatly modified by changing the exchange interaction and the transverse field. Additionally, the influence of particle size on static and dynamic properties of ferroelectric nanoparticles was evaluated convincingly by Wang *et al.*[20] and Michael *et al.*[21,22] In many theoretical investigations of ferroelectric thin films using TIM, the size effect is only studied along the thickness direction, yet the lateral size effect has not been considered. Motivated by this, Xin *et al.*[23] systematically studied the lateral size-drive phase transformation in a monolayer ferroelectric square lattice. It is indicated that the Curie temperature and the polarization of the lattice depend sensitively on its lateral size when the size becomes very small, and a phase transformation from ferroelectric phase to paraelectric phase occurs with the weakening of the long-range interaction in the lattice.

According to the investigations mentioned above, it has been demonstrated that the lateral and thickness size effects both play a crucial role in determining the ferroelectric characteristics of a small size film. Although Xin *et al.*[23] studied lateral size effect in a monolayer ferroelectric square lattice, the thickness direction size effect has not been taken into account in that investigation. In experiments, variations in the lateral and thickness sizes can lead to many interesting phenomena. Up to now, ferroelectric properties of a film with

a)Electronic mail: ltq@hit.edu.cn.

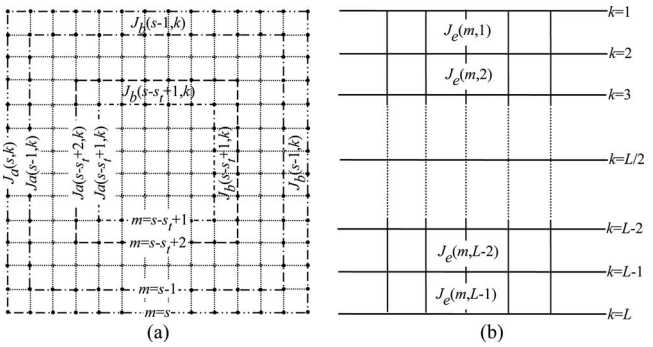

FIG. 1. Schematic illustration of the ferroelectric thin film with $N\times N\times L$ size. (a) The distribution of the square loop in the pseudospin plane. (b) The distribution of the pseudospin layer along the z direction.

finite size in three dimensions have not been studied using the TIM. Furthermore, in many theoretical studies on ferroelectric thin films using the TIM, the structural difference between surface layers and the interior of the thin film is expressed by modifying the two pseudospin interaction J_{ij} and the transverse field Ω_i, namely, J_{ij} and Ω_i in surface layers are assumed identical and only differ from those of the interior. It means that the structural variation from surface layers to the interior of the thin film is only a "single-step" change. In reality, the structural change is gradual and continuous due to diffusion. Therefore, it is not practical to utilize a single-step model to study ferroelectric characteristics of a finite size film. In order to better reflect realistic structure of ferroelectric thin films of finite size, it is necessary to introduce inhomogeneous structural transition zones in both the lateral and thickness directions.[12]

In this paper, adopting the Fermi-type Green's function technique, we have introduced a multistep structural change near the lateral edges and the surfaces of the film in the TIM to study the influence of the structural transition zones and the film size on the polarization and the Curie temperature in the ferroelectric thin film.

II. THE MODEL

Schematic of a finite size ferroelectric thin film with two symmetrical surfaces is shown in Fig. 1. All pseudospin layers are parallel to the x-y plane and the pseudospins are located at the square grid points. The z-direction is perpendicular to the film surface and is also the polarization direction. The film volume is $N\times N\times L$, where N and L represent the lateral and the thickness dimensions of the film, respectively. In Fig. 1(a), every pseudospin layer is divided into a series of square loops, whose size gradually becomes smaller from the outside to the center. The location of each square loop is labeled by $m=1,2,\ldots,s$, where s [$s=N/2$ or $(N+1)/2$] is the number of square loops in a pseudospin layer, $m=s$ stands for the edge loop, and s_t represents the number of transition square loops in the lateral edge zone of the film, including the edge loop. In Fig. 1(b), the position of each pseudospin layer is labeled by $k=1,2,\ldots,L$, where $k=1$ and $k=L$ denote the surface layers of the film along the z-direction.

The system is described by the Ising Hamiltonian under a transverse field,[24]

$$H=-\sum_i \Omega_i s_i^x-\sum_{ij} J_{ij}s_i^z s_j^z, \tag{1}$$

where Ω_i is the transverse field at site i, s_i^x and s_i^z are the x and z components of a spin-1/2 operator at site i, J_{ij} is the exchange interaction between sites i and j, and the sum Σ_{ij} runs over only the nearest-neighbor pairs. $J_{ij}=J_a(m,k)$ if sites i and j locate in the same square loop (m is fixed); $J_{ij}=J_b(m,k)$ if the two sites are in the mth and the $(m+1)$th square loops, respectively; and $J_{ij}=J_e(m,k)$ if the two sites situate in the kth and the $(k+1)$th pseudospin layers, respectively.

So far there are no available experimental data on structural transition zones; therefore, we use simple distribution functions to indicate their characteristics. It must be noted that the forms of the distribution functions do not influence the generality of the results and conclusions.[12] In light of the above argument, the exponential function is introduced to characterize the inhomogeneous structural distribution near the edge of a film. For simplicity, it is assumed that the film is symmetric along the z-direction. So the expressions of exchange interaction J_{ij} for the upper film containing $L/2$ [or $(L+1)/2$ including the middle layer] layers can be expressed as

$$J_a(m,k)=J_\infty e^{-1/(\alpha_1\times N\times L\times k)},\quad 1\le m\le (s-s_t),\quad 1\le k\le L/2,\quad \text{or}\quad 1\le k\le (L+1)/2, \tag{2a}$$

$$J_a(m,k)=J_s e^{-1/(\alpha_1\times N\times L\times k)},\quad m=s,\quad 1\le k\le L/2\quad \text{or}\quad 1\le k\le (L+1)/2, \tag{2b}$$

$$J_a(m,k)=J_a(s,k)+[J_a(2,k)-J_a(s,k)]\times(1-e^{-\beta_1(m_t-1)/s_t}),\quad m=s+1-m_t,\quad 1\le m_t\le s_t,\quad 1\le k\le L/2,\quad \text{or}\quad 1\le k\le (L+1)/2, \tag{2c}$$

$$J_b(m,k)=J_\infty e^{-1/(\alpha_1\times N\times L\times k)},\quad 1\le m\le (s-s_t),\quad 1\le k\le L/2,\quad \text{or}\quad 1\le k\le (L+1)/2, \tag{3a}$$

$$J_b(m,k)=J_a(s,k)+[J_a(2,k)-J_a(s,k)]\times(1-e^{-\beta_2 m_t/s_t}),\quad m=s-m_t,\quad 1\le m_t\le (s_t-1),\quad 1\le k\le L/2,\quad \text{or}\quad 1\le k\le (L+1)/2, \tag{3b}$$

$$J_e(m,k)=J_\infty e^{-1/(\alpha_2\times N\times L\times k)},\quad 1\le m\le (s-s_t),\quad 1\le k\le L/2,\quad \text{or}\quad 1\le k\le (L+1)/2, \tag{4a}$$

$$J_e(m,k)=J_{es} e^{-1/(\alpha_2\times N\times L\times k)},\quad m=s,\quad 1\le k\le L/2\quad \text{or}\quad 1\le k\le (L+1)/2, \tag{4b}$$

$$J_e(m,k) = J_e(s,k) + [J_e(1,k) - J_e(s,k)] \times (1 - e^{-\beta_3(m_t-1)/s_t}), \quad m = s+1-m_t, \quad 1 \le m_t \le s_t, \quad 1 \le k \le L/2, \quad \text{or} \quad 1 \le k \le (L+1)/2, \tag{4c}$$

where m_t labels the position of each transition square loop, J_∞ represents the interaction between two nearest-neighbor pseudospins in an infinite pseudospin plane, J_s and J_{es} are the interaction between the pseudospins in the same edge loop and in different layers when the film thickness is infinite and when $m=s$, β_1 (β_2) is the interaction intensity parameter when the two pseudospins situate in the same (different) transition square loop, β_3 is the interaction intensity parameter when the two pseudospins locate in different layers and in the lateral structural transition zone, and α_1 (α_2) denotes the interaction intensity parameter when the two pseudospins do not locate in the lateral structural transition zone but in the same (different) layer. For thin film, it is known that the magnitude of dipole moments enlarges with the increase in the film size. Hence, a reasonable hypothesis is that the exchange interaction is enhanced with the increase in the film size. Also, the two pseudospin interactions gradually change from the surface layer to the interior of the thin film due to the inhomogeneous structural distribution along the thickness direction. Additionally, $J_a(1,k)=0$ if the lateral size N is an odd number.

The retarded Green's function for the Fermi-type annihilation operator $a_{i\sigma}$ and the creation operator $a_{i\sigma}^+$ of the pseudospin at site i is defined by[24]

$$\langle\langle a_{i\sigma}(t)|a_{i\sigma}^+(0)\rangle\rangle = i\theta(t)\langle[a_{i\sigma}(t),a_{i\sigma}^+(0)]_+\rangle. \tag{5}$$

The Fourier-transformed Green's function satisfies the following equation of motion (corresponding to the time t):

$$\omega\langle\langle a_{i\sigma}|a_{i\sigma}^+\rangle\rangle(\omega) = \langle[a_{i\sigma},a_{i\sigma}^+]_+\rangle + \langle\langle[a_{i\sigma},H]|a_{i\sigma}^+\rangle\rangle(\omega). \tag{6}$$

By substituting Eq. (1) into Eq. (6), we can obtain

$$\omega\langle\langle a_{i\sigma}|a_{i\sigma}^+\rangle\rangle(\omega) = 1 - \Omega_i\langle\langle a_{i-\sigma}|a_{i\sigma}^+\rangle\rangle(\omega) - \sum_j J_{ij}\langle\langle S_j^z a_{i\sigma}|a_{i\sigma}^+\rangle\rangle(\omega), \tag{7}$$

$$\omega\langle\langle a_{i-\sigma}|a_{i\sigma}^+\rangle\rangle(\omega) = -\Omega_i\langle\langle a_{i\sigma}|a_{i\sigma}^+\rangle\rangle(\omega) + \sum_j J_{ij}\langle\langle S_j^z a_{i-\sigma}|a_{i\sigma}^+\rangle\rangle(\omega). \tag{8}$$

Applying the simple decoupling method, the higher-order Green's function in the above equations may be approximately expressed as

$$\langle\langle S_j^z a_{i\sigma}|a_{i\sigma}^+\rangle\rangle(\omega) \approx \langle S_j^z\rangle\langle\langle a_{i\sigma}|a_{i\sigma}^+\rangle\rangle(\omega), \tag{9}$$

$$\langle\langle S_j^z a_{i-\sigma}|a_{i\sigma}^+\rangle\rangle(\omega) \approx \langle S_j^z\rangle\langle\langle a_{i-\sigma}|a_{i\sigma}^+\rangle\rangle(\omega). \tag{10}$$

Utilizing Eqs. (7)–(10), the Green's function can be obtained as follows:

$$\langle\langle a_{i\sigma}|a_{i\sigma}^+\rangle\rangle(\omega) = \frac{\omega - \delta_i}{\omega^2 - \omega_i^2}, \tag{11}$$

$$\langle\langle a_{i-\sigma}|a_{i\sigma}^+\rangle\rangle(\omega) = \frac{-\Omega_i}{\omega^2 - \omega_i^2}, \tag{12}$$

where

$$\delta_i = \sum_j J_{ij}\langle S_j^z\rangle, \tag{13a}$$

$$\omega_i^2 = \Omega_i^2 + \delta_i^2. \tag{13b}$$

Hence, the transcendental equation with respect to the thermal average $\langle S_i^z\rangle$ and $\langle S_i^x\rangle$ at site i can be written as

$$\langle S_i^z\rangle = (\delta_i/2\omega_i)\tanh(\omega_i/2k_BT), \tag{14}$$

$$\langle S_i^x\rangle = (\Omega_i/2\omega_i)\tanh(\omega_i/2k_BT), \tag{15}$$

where k_B is the Boltzmann constant and T is the absolute temperature. Evidently, it is the result of the usual mean-field approximation (MFA), which means that the simple decoupling approximation coincides completely with the usual MFA. Adopting the simple decoupling approximation, the result of MFA can also be obtained by spin operators.[27] However, the higher-order Green's function can be more easily formulated with the aid of Fermi-type operators.[24] In this paper, the result of the simple decoupling approximation is employed. Additionally, using the simple decoupling approximation, the result of MFA can also be obtained by the drone-fermion representation[28–30] (see the Appendix). That is to say, by applying the simple decoupling approximation to the higher-order Green's function, the same result can be obtained with the help of the drone-fermion representation and Fermi-type operators.

The polarization P_i at site i is proportional to $\langle S_i^z\rangle$ in the absence of applied electric field E, namely,

$$P_i = 2n\mu\langle S_i^z\rangle, \tag{16}$$

where n is the number of pseudospins in a unit volume and μ is the dipole moment of the pseudospin. Consequently, the mean polarization of a finite size film is given by

$$\bar{P} = \frac{1}{(N^2\times L)}\sum_{i=1}^{N^2\times L} P_i = \frac{2n\mu}{(N^2\times L)}\sum_{i=1}^{N^2\times L}\langle S_i^z\rangle. \tag{17}$$

When T approaches the Curie temperature, the pseudospin average tends to be zero so that Eq. (14) can be reduced to

$$\sum_j J_{ij}\langle S_j^z\rangle - [2\Omega_i/\tanh(\Omega_i/2k_BT)]\langle S_i^z\rangle = 0. \tag{18}$$

Equation (18) represents a set of linear equations from which the Curie temperature can be determined by its coefficient determinant. For a bulk material with a second-order phase transformation, the transverse field Ω_i and the exchange interaction J_{ij} are constant. The Curie temperature T_b can be obtained from the following equation:[25]

$$\tanh(\Omega/2k_BT_b) = 2\Omega/rJ, \tag{19}$$

where J is the nearest-neighbor interaction and r is the coordination number. In our calculations, the corresponding vari-

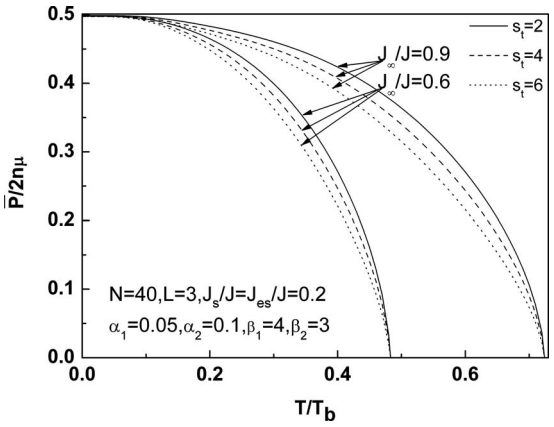

FIG. 2. The mean polarization of the film as a function of the temperature with different s_t and J_∞.

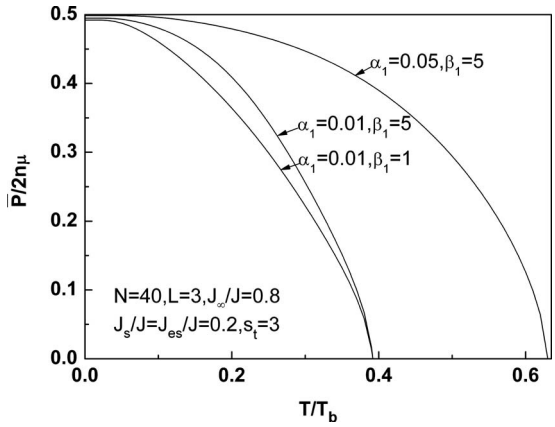

FIG. 3. The temperature dependence of the mean polarization of the film with different α_1 and β_1.

ables are renormalized to dimensionless units by utilizing the bulk material parameters.

III. NUMERICAL RESULTS AND DISCUSSIONS

In this section, we present numerical results based on Eqs. (17) and (18). For simplicity, the transverse field at all sites is treated identically in our calculations, and we assign $\Omega_i/J=0.1$ and set $\beta_3=\beta_1$.

Figure 2 shows the dependence of the mean polarization of the thin film on temperature T/T_b with different s_t and J_∞. The mean polarization decreases markedly with the increase in s_t when J_∞/J is fixed (e.g., $J_\infty/J=0.9$). However, the Curie temperature of the film does not change with the enhancement of s_t. On the other hand, the mean polarization and the Curie temperature of the film are both increased with the increase in J_∞ when s_t is fixed (e.g., $s_t=2$). The reason is that the Curie temperature is mainly determined by the interaction intensity near the center of the film for a fixed size film, and the pseudospin interaction is strengthened everywhere except the edge loop with the increase in J_∞. Evidently, the strengthened interaction between the pseudospins contributes to the stabilization of the ferroelectricity in the film. In summary, the number of transition square loops influences the polarization rather than the Curie temperature, whereas J_∞ affects both the polarization and the Curie temperature when the film dimensions are fixed.

Figure 3 presents the mean polarization of the film as a function of temperature T/T_b for several different interaction intensity parameters. For convenience of discussion, we set $\alpha_2=\alpha_1$ and $\beta_2=\beta_1$. From Fig. 3, it can be seen that the mean polarization decreases with the reduction in β_1, but the Curie temperature of the thin film is insensitive to the change in β_1 when α_1 is fixed (here $\alpha_1=0.01$). This is because β_1 can only change the interaction intensities in the lateral structure transition zone but not near the center of the film. On the other hand, the mean polarization and the Curie temperature of the thin film both decrease with the reduction in α_1 when β_1 is fixed (here $\beta_1=5$). The reason is that the interaction intensities near the center of the film are weakened with the decrease in α_1. Based on the results in Figs. 2 and 3, the structural transition zone near the lateral edge of the film, characterized by the number of the transition square loops and the interaction intensity parameters β_1 and β_2, only affects the polarization, but J_∞ and interaction intensity parameters α_1 and α_2 influence both the mean polarization and the Curie temperature of the film. This microscopic nature that determines the polarization and the Curie temperature of the film cannot be obtained from the phenomenological Landau theory.[11]

The mean polarization of the film versus temperature curves for different film sizes are shown in Fig. 4. One can see from Fig. 4 that the mean polarization and the Curie temperature are strongly influenced by the lateral and thickness dimensions of the film. The mean polarization and the Curie temperature both increase with the increase in size along the lateral and thickness directions of the film. This can be ascribed to the fact that the number of the pseudospins contributing to the ferroelectricity of the film increases with the increase in the film size. Therefore, the two pseudospin effective interactions in the film are strengthened. Our results are in agreement with previous theoretical results[11,21] and experimental data of small $PbTiO_3$ (PTO) (Refs. 4–6) and $BaTiO_3$ (BTO) (Ref. 7) particles. In Fig. 4 we show the results for the cases of $N=40$ and $N=\infty$ with fixed film thickness $L=4$. The mean polarization and the Curie temperature both increase noticeably when the lateral size changes from a finite value to infinity. The comparison between the bulk material and the finite size thin film shows the

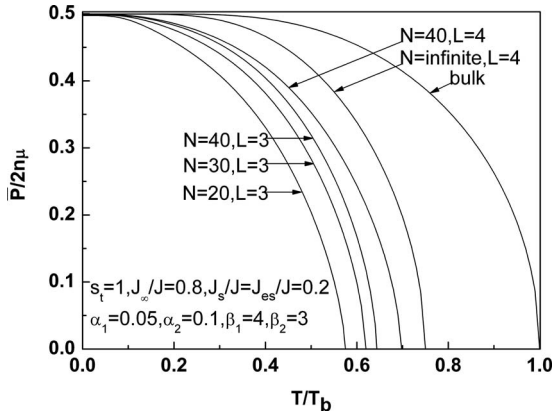

FIG. 4. The mean polarization of the film as a function of the temperature with different N and L.

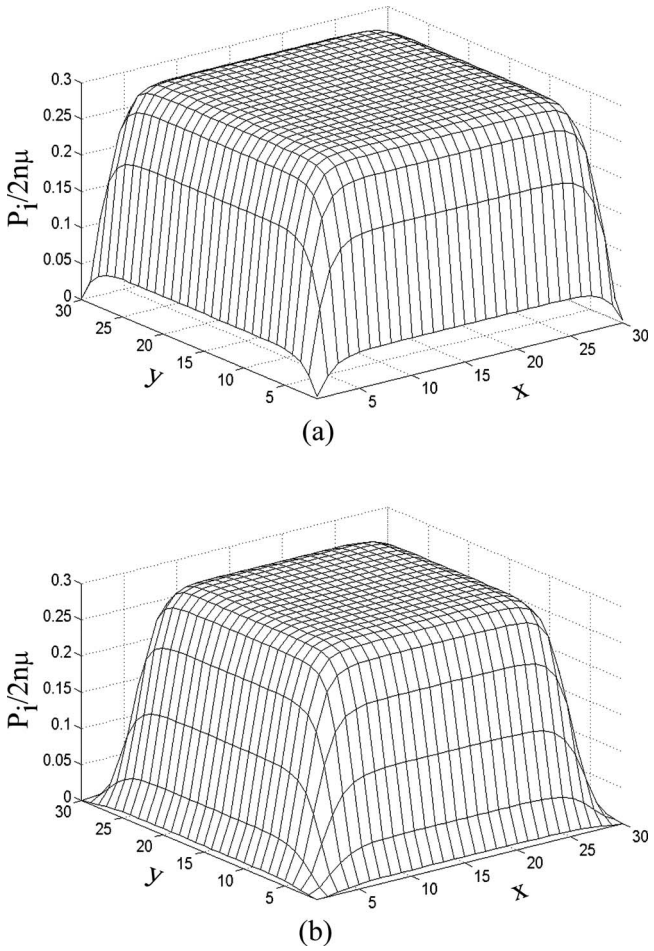

FIG. 5. The spatial distribution of the polarization for the second layer of the film: (a) $s_t=1$ and (b) $s_t=4$. The parameters concerned in the calculation are $N=30$, $L=4$, $T/T_b=0.6$, $J_s/J=J_{es}/J=0.2$, $J_\infty/J=0.8$, $\alpha_1=0.05$, $\alpha_2=0.1$, $\beta_1=4$, and $\beta_2=3$.

same tendency. This is understandable because the two pseudospin interactions for a finite size film are weaker than those of infinite size film.

Figure 5 shows the spatial distribution of the polarization for the second layer ($k=2$) of the film with different s_t. In Fig. 5(a), it is shown that the polarization near the center zone of the second layer of the film has almost no change and reaches the maximum value. The magnitude of the polarization near the film boundary drops sharply. Our results are qualitatively in agreement with theoretical result[11,23] and could qualitatively explain the decrease in the polarization in small particles of PTO (Refs. 4 and 5) and BTO.[7] In addition, Fig. 5(b) shows that the polarization reduction extends into the interior of the film with the widening of the lateral structural transition zone of the film.

Figure 6 presents the relation of the lateral size of the film to the Curie temperature for several different film thicknesses. It is demonstrated that the Curie temperature of the film decreases to zero when the thin film size shrinks below a critical value, i.e., a size-driven phase transformation will occur. It gives the critical lateral size when the film thickness is fixed. One can also see that thicker film corresponds to smaller critical lateral size because the thicker is the film, the stronger is the interlayer interaction, which means that the

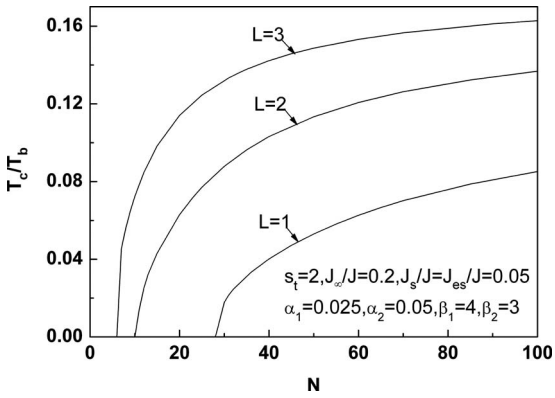

FIG. 6. The Curie temperature depending on the lateral size of the film with different film thicknesses.

ferroelectricity of the film can persist down to a smaller lateral size. On the other hand, thicker film also leads to higher Curie temperature when the lateral size of the film is fixed. Likewise, larger lateral size of the film is responsible for higher Curie temperature when the film thickness is defined. In addition, for a three-layer film, the Curie temperature increases and slows down with the increase in the lateral size when $N>50$, which is in qualitative agreement with the available experimental results of PTO (Refs. 5 and 6) and BTO (Ref. 7) nanostructures. It means that the lateral size of the film has a notable influence on the Curie temperature for a small size film, which confirmed the conclusion reported in Refs. 11 and 23.

The Curie temperature of the film as a function of α_1 with different J_∞ is shown in Fig. 7. Here we set $\alpha_2=\alpha_1$. In the case of $J_\infty/J=0.8$, the Curie temperature of the film decreases sharply to zero with the reduction in α_1, which means that a phase transformation has taken place. This is indicative of the fact that the interaction between the pseudospins is so weak that the ferroelectricity of the film is unstable for a film with fixed size. Furthermore, the Curie temperature of the film increases slowly with the enhancement of α_1 when $\alpha_1>0.2$. The reason is that the interaction between the pseudospins is enhanced slowly with the increase in α_1 in this case. The trend can also be found in other curves in Fig. 7. Comparing the three curves in Fig. 7, one

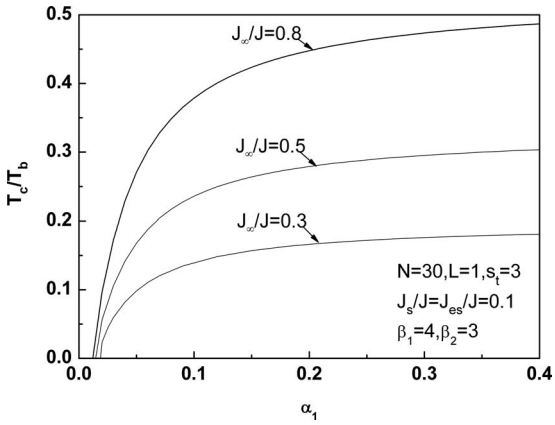

FIG. 7. The parameter α_1 dependence of the Curie temperature of the film with different J_∞.

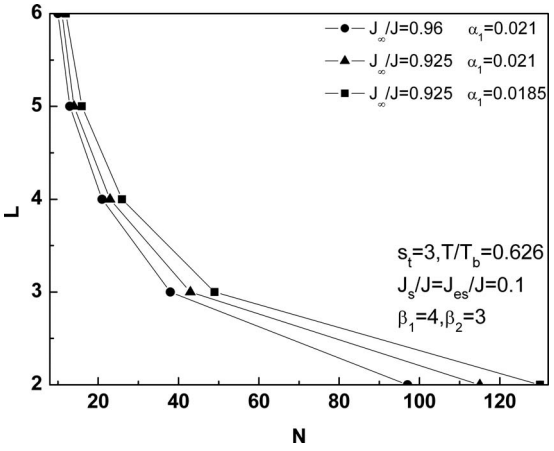

FIG. 8. The critical lateral size dependence of the critical film thickness with different J_∞ and α_1.

can see that the critical value of α_1 varies with J_∞, namely, the smaller is the parameter J_∞, the larger is the critical value of α_1. Additionally, the Curie temperature shifts to lower-temperature region with the decrease in J_∞ when α_1 is defined.

Figure 8 depicts the critical size of the film with different parameters J_∞ and α_1 (we set $\alpha_2=\alpha_1$). One can see that the thinner is the film, the larger is the critical lateral size when other parameters are defined, and vice versa. The critical size of the film is reduced with the increase in α_1 when J_∞ is a constant (here $J_\infty/J=0.925$). Likewise, the critical size of the film decreases with the increase in J_∞ when α_1 is fixed (here $\alpha_1=0.021$). This is indicative of the fact that stronger interaction between the pseudospins leads to smaller critical size of the film.

IV. SUMMARY AND CONCLUSIONS

In summary, the phase transformation properties of the ferroelectric thin film with finite size in three dimensions have been investigated by a modified TIM using the Fermi-type Green's function technique. The results can be summarized as follows. (1) The influence of the structural transition zone near the film lateral edge on the phase transformation properties cannot be neglected for a finite size film. The wider is the lateral structural transition zone (more transition square loops) and the weaker is the interaction intensities in this region, the smaller is the mean polarization of the film, but the Curie temperature is not affected. (2) The interaction intensities near the center of film determine the polarization as well as the Curie temperature for a fixed size film. The mean polarization and the Curie temperature both decrease with the weakening of the interaction near the center of the film. (3) The lateral size and the thickness of the film both affect the phase transformation properties of the film for a small size film. The thinner is the film, the larger is the critical lateral size.

Because the dependence of the phase transformation properties on the lateral size of the film becomes more important for a smaller size film, our theoretical investigation here provides some useful guidance to the effort of miniaturization of thin film based electronic devices.

APPENDIX: THE MFA FROM THE DRONE-FERMION REPRESENTATION

The spin operators satisfy the commutation rules

$$[S_i^+, S_j^-]_- = 2\delta_{ij} S_i^z, \tag{A1a}$$

$$[S_i^z, S_j^\pm]_- = \pm \delta_{ij} S_i^\pm, \tag{A1b}$$

$$[S_i^+, S_j^-]_+ = 1, \tag{A1c}$$

where $S^+=S^x+iS^y$ and $S^-=S^x-iS^y$. From Eq. (A1c), we note that the spin operators behave like fermions for spin-1/2. They can be conveniently expressed by the drone-fermion representation, i.e., a pair of fermion operators c_i and d_i,

$$S_i^z = c_i^+ c_i - \tfrac{1}{2}, \tag{A2a}$$

$$S_i^+ = c_i^+ \phi_i, \tag{A2b}$$

$$\phi_i = d_i + d_i^+. \tag{A2c}$$

The complete anticommutation rules are

$$[c_i, c_j^+]_+ = [d_i, d_j^+]_+ = \delta_{ij}. \tag{A3}$$

All other pairs of operators anticommute.

The equations of motion for the Green's function can be derived in accordance with the Hamiltonian of the TIM,

$$\omega\langle\langle c_i|c_i^+\rangle\rangle(\omega) = 1 - \frac{\Omega_i}{2}\langle\langle \phi_i|c_i^+\rangle\rangle(\omega) - \sum_j J_{ij}\langle\langle S_j^z c_i|c_i^+\rangle\rangle(\omega), \tag{A4}$$

$$\omega\langle\langle \phi_i|c_i^+\rangle\rangle(\omega) = \Omega_i\langle\langle c_i^+|c_i^+\rangle\rangle(\omega) - \Omega_i\langle\langle c_i|c_i^+\rangle\rangle(\omega), \tag{A5}$$

$$\omega\langle\langle c_i^+|c_i^+\rangle\rangle(\omega) = \frac{\Omega_i}{2}\langle\langle \phi_i|c_i^+\rangle\rangle(\omega) + \sum_j J_{ij}\langle\langle S_j^z c_i^+|c_i^+\rangle\rangle(\omega). \tag{A6}$$

Adopting the simple decoupling scheme to the higher-order Green's functions, they can be approximated as

$$\langle\langle S_j^z c_i|c_i^+\rangle\rangle(\omega) \approx \langle S_j^z\rangle\langle\langle c_i|c_i^+\rangle\rangle(\omega), \tag{A7}$$

$$\langle\langle S_j^z c_i^+|c_i^+\rangle\rangle(\omega) \approx \langle S_j^z\rangle\langle\langle c_i^+|c_i^+\rangle\rangle(\omega). \tag{A8}$$

Utilizing Eqs. (A4)–(A8), the Green's function can be obtained as follows:

$$\langle\langle c_i|c_i^+\rangle\rangle(\omega) = \frac{2\omega^2 - 2\omega\delta_i - \Omega_i}{2\omega(\omega^2 - \omega_i^2)}, \tag{A9}$$

$$\langle\langle \phi_i|c_i^+\rangle\rangle(\omega) = \frac{-\Omega_i(\omega - \delta_i)}{\omega(\omega^2 - \omega_i^2)}, \tag{A10}$$

$$\langle\langle c_i^+|c_i^+\rangle\rangle(\omega) = \frac{-\Omega_i^2}{2\omega(\omega^2 - \omega_i^2)}, \tag{A11}$$

where

$$\delta_i = \sum_j J_{ij}\langle S_j^z\rangle, \tag{A12a}$$

$$\omega_i^2 = \Omega_i^2 + \delta_i^2. \tag{A12b}$$

The correlation functions $\langle c_i^+ c_i \rangle$ and $\langle c_i^+ \phi_i \rangle$ are gained by the spectral theorem

$$\langle c_i^+ c_i \rangle = 1/2 + (\delta_i/2\omega_i)\tanh(\omega_i/2k_BT), \tag{A13}$$

$$\langle c_i^+ \phi_i \rangle = (\Omega_i/2\omega_i)\tanh(\omega_i/2k_BT). \tag{A14}$$

Hence, the transcendental equation with respect to the thermal average $\langle S_i^z \rangle$ and $\langle S_i^x \rangle$ at site i can be written as

$$\langle S_i^z \rangle = \langle c_i^+ c_i \rangle - 1/2 = (\delta_i/2\omega_i)\tanh(\omega_i/2k_BT), \tag{A15}$$

$$\langle S_i^x \rangle = \langle c_i^+ \phi_i \rangle = (\Omega_i/2\omega_i)\tanh(\omega_i/2k_BT), \tag{A16}$$

where k_B is the Boltzmann constant and T is the absolute temperature. Evidently, it is the result of the usual MFA.

[1] M. Dawber, K. M. Rabe, and J. F. Scott, Rev. Mod. Phys. **77**, 1083 (2005).
[2] I. Stolichnov, E. Colla, A. Tagantsev, S. S. N. Bharadwaja, S. Hong, N. Setter, J. S. Cross, and M. Tsukada, Appl. Phys. Lett. **80**, 4804 (2002).
[3] D. J. Kim, J. Y. Jo, Y. W. So, B. S. Kang, T. W. Noh, J.-G. Yoon, T. K. Song, K. H. Noh, S.-S. Lee, S.-H. Oh, K.-N. Lee, S.-K. Hong, and Y.-J. Park, Appl. Phys. Lett. **86**, 022903 (2005).
[4] S. Chattopadhyay, P. Ayyub, V. R. Palkar, and M. Multani, Phys. Rev. B **52**, 13177 (1995).
[5] W. L. Zhong, B. Jiang, P. L. Zhang, J. M. Ma, H. M. Chen, Z. H. Yang, and L. X. Li, J. Phys.: Condens. Matter **5**, 2619 (1993).
[6] K. Ishikawa, K. Yoshikawa, and N. Okada, Phys. Rev. B **37**, 5852 (1988).
[7] T. Ohno, D. Suzuki, K. Ishikawa, M. Horiuchi, T. Matsuda, and H. Suzuki, Ferroelectrics **337**, 25 (2006).
[8] D. D. Fong, A. M. Kolpak, J. A. Eastman, S. K. Streiffer, P. H. Fuoss, G. B. Stephenson, C. Thompson, D. M. Kim, K. J. Choi, C. B. Eom, I. Grinberg, and A. M. Rappe, Phys. Rev. Lett. **96**, 127601 (2006).
[9] K. Lee and S. Baik, Appl. Phys. Lett. **86**, 202901 (2005).
[10] K. Lee, H. Yi, W.-H. Park, Y. K. Kim, and S. Baik, J. Appl. Phys. **100**, 051615 (2006).
[11] Y. G. Wang, W. L. Zhong, and P. L. Zhang, Phys. Rev. B **51**, 17235 (1995).
[12] T. Q. Lü and W. W. Cao, Phys. Rev. B **66**, 024102 (2002).
[13] A. M. Bratkovsky and A. P. Levanyuk, Phys. Rev. Lett. **94**, 107601 (2005).
[14] R. Ahluwalia and D. J. Srolovitz, Phys. Rev. B **76**, 174121 (2007).
[15] Q. Y. Qiu and V. Nagarajan, J. Appl. Phys. **102**, 104113 (2007).
[16] I. I. Naumov, L. Bellaiche and H. Fu, Nature (London) **432**, 737 (2004).
[17] Y.-H. Tang and M.-H. Tsai, J. Appl. Phys. **103**, 034305 (2008).
[18] J. M. Wesselinowa and S. Trimper, Phys. Status Solidi B **241**, 1141 (2004).
[19] Y. Xiong, K. Xiao-Yu, and L. Cheng, Solid State Commun. **139**, 397 (2006).
[20] C. L. Wang, Y. Xin, X. S. Wang, and W. L. Zhong, Phys. Rev. B **62**, 11423 (2000).
[21] Th. Michael, S. Trimper, and J. M. Wesselinowa, Phys. Rev. B **76**, 094107 (2007).
[22] Th. Michael, S. Trimper, and J. M. Wesselinowa, Phys. Rev. B **74**, 214113 (2006).
[23] Y. Xin, C. L. Wang, W. L. Zhong, and P. L. Zhang, Phys. Lett. A **260**, 411 (1999).
[24] B. H. Teng and H. K. Sy, Phys. Rev. B **70**, 104115 (2004).
[25] X. G. Wang, S. H. Pan, and G. Z. Yang, J. Phys.: Condens. Matter **11**, 6581 (1999).
[26] A. Tabyaoui, M. Madani, A. Ainane, and M. Saber, Physica A **358**, 150 (2005).
[27] V. Ramakrishnan and T. Tanaka, Phys. Rev. B **16**, 422 (1977).
[28] G. D. Houston, and H. C. Bolton, J. Phys. C **4**, 2097 (1971).
[29] G. D. Houston, and H. C. Bolton, J. Phys. C **4**, 2894 (1971).
[30] D. P. Chock, P. Résibois, G. Dewel, and R. Dagonnier, Physica (Utrecht) **53**, 364 (1970).